# Isolation of Components due to Intracortical Processing in the Visual Evoked Potential

Jonathan D. Victor

*Proceedings of the National Academy of Sciences of the United States of America*, Volume 83, Issue 20 (Oct. 15, 1986), 7984-7988.

Stable URL:
http://links.jstor.org/sici?sici=0027-8424%2819861015%2983%3A20%3C7984%3AIOCDTI%3E2.0.CO%3B2-S

*Proc. Natl. Acad. Sci. USA*
Vol. 83, pp. 7984–7988, October 1986
Neurobiology

# Isolation of components due to intracortical processing in the visual evoked potential

(receptive fields/pattern processing/isodipole textures/nonlinear systems)

JONATHAN D. VICTOR

Laboratory of Biophysics, The Rockefeller University, 1230 York Avenue, New York, NY 10021

*Communicated by Floyd Ratliff, June 27, 1986*

**ABSTRACT** **A class of stochastic visual textures are used to analyze the components of the visual evoked potential (VEP). This procedure exploits the differential sensitivity of populations of visual neurons to aspects of contrast and pattern. A simple transformation of VEP responses elicited by these stimuli separates components that reflect complex aspects of visual processing from those that reflect elementary aspects. Simultaneous recordings of the VEP and cellular activity in the cat lateral geniculate nucleus are obtained. Responses to traditional VEP stimuli contain a mixture of intracortically generated and precortically generated components. A theoretical and experimental analysis demonstrates that the present approach cleanly separates intracortical generators of the VEP from precortical generators.**

The physiological basis of cerebral processing of sensory information is the electrical activity of individual neurons. The evoked potential, an averaged electroencephalographic signal recorded over the scalp, is an indirect manifestation of this electrical activity, which contains contributions from many functionally distinct classes of neurons (1–3).

The present approach to the analysis of visual evoked potential (VEP) components exploits a class of stochastic visual textures, the isodipole texture pairs (4). Isodipole texture pairs, which have the same second-order correlation statistics, have spatial frequency spectra of identical amplitudes. Thus, the ability to distinguish these textures must be due to pattern processing, which is more complex than spatial frequency analysis or any other linear process (5, 6). Similarly, antisymmetric VEP components recorded during interchange of these isodipole textures must reflect complex spatial processing. Such antisymmetric VEP components have a longer latency and slower dynamics than contrast–reversal or appearance–disappearance VEPs.* On the basis of the known properties of retinal ganglion cells and lateral geniculate nucleus (LGN) neurons, it was hypothesized that these VEP components result from intracortical processing (5, 6).

The VEP is an average of electrical activity over a wide area of cortex. To compare the VEP with single-unit activity, a modification of the isodipole texture technique is introduced in which the implicit spatial average is replaced by an explicit temporal average. The new stimulus permits experimental confirmation that the isodipole texture paradigm cleanly isolates intracortical processes in the antisymmetric component of the VEP.

## METHODS

**Stimulus Description.** The visual stimuli used in these studies consist of alternation between examples of the "even" and "odd" isodipole textures introduced by Julesz *et al.* (4) in psychophysical studies. Fig. 1 shows small samples of each texture: a portion of the even texture in the lower plane and a portion of the odd texture in the upper plane. The squares of the first row and column of the texture may be chosen arbitrarily; the remainder of the squares are defined by a recursive procedure. In the even texture, only an even number (0, 2, or 4) of squares of each color meet at every corner; in the odd texture, an odd number (1 or 3) of squares of each color meet at every corner.

An even texture may be converted into an odd texture by reversing the state of some of the squares and keeping the others constant. For example, reversal of the squares that lie at the intersection of an odd-numbered row and an odd-numbered column will interconvert even and odd textures of Fig. 1. The squares whose states change are connected by the vertical arrows of Fig. 1.

The present visual stimulus (the isodipole-16 stimulus) consists of abrupt alternation between 1 of 8 examples of the even texture, and 1 of 8 examples of the odd texture. Each presentation of an even texture is followed by a presentation of an odd texture and vice-versa, but the specific even and odd texture is chosen at random. All 16 textures are presented an equal number of times, and all possible transitions from a given even texture to a given odd texture are presented an equal number of times.

The 16 even and odd textures are all derived from a single even texture as shown in Fig. 2. All squares of the lattice are partitioned into four sets, labeled A, B, C, and D (*Inset*). Reversal of the state of any 1 set of the squares converts an even texture into an odd texture. For example, the even texture of Fig. 1 corresponds to the upper texture of Fig. 2. Reversal of the squares labeled A in the *Inset* results in the conversion to the odd texture of Fig. 1, which corresponds to the texture labeled A in Fig. 2. Reversal of the state of 1 of the other 3 sets (B, C, or D) results in the other 3 odd textures of the second row of Fig. 2. Similarly, reversal of any 2 of the sets of squares changes the even texture into 1 of 6 additional even textures (1 for each of the 6 possible pairs, AB, AC, AD, BC, BD, and CD). Reversal of exactly 3 of the 4 sets again results in 4 more odd textures, and reversal of all 4 of the squares produces an 8th even texture. In an experiment using the isodipole-16 stimulus, the average response to each of the 8 textures that comprise the even phase of the isodipole-16 stimulus is compared to the averaged response to each of the 8 textures of the odd phase.

Considered as two ensembles, the set of 8 even textures and the set of 8 odd textures have the following properties: within each group, every square of the stimulus is white exactly half of the time. Furthermore, each possible pairwise configuration of squares (black next to black, white next to

The publication costs of this article were defrayed in part by page charge payment. This article must therefore be hereby marked "*advertisement*" in accordance with 18 U.S.C. §1734 solely to indicate this fact.

Abbreviations: VEP, visual evoked potential; LGN, lateral geniculate nucleus.

*Victor, J. D., Proceedings of the 7th Annual Conference of the Institute of Electrical and Electronics Engineers Engineering in Medicine and Biology Society, Sept. 27–30, 1985, Chicago, pp. 420–425.

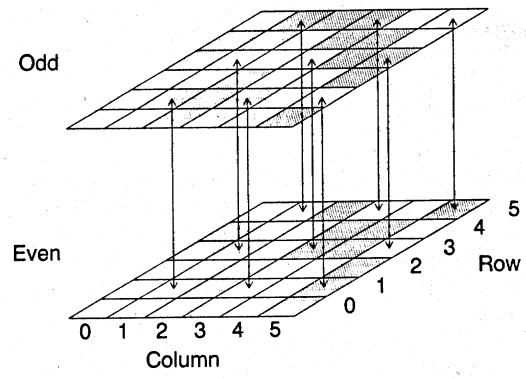


FIG. 1. Diagram of the construction of even and odd textures. Each plane illustrates a portion of one of the two textures. Open squares have a luminance above the mean; hatched squares have a luminance the same distance below the mean. Three-quarters of the squares are at the same luminance in both textures. The remaining one-quarter of the squares, at the intersection of an odd-numbered row and an odd-numbered column, are in opposite states. These squares are connected by the vertical arrows.

white, black next to white, and white next to black) occurs the same number of times (twice) in each of the 2 sets. A similar result holds for pairs of squares that are not nearest neighbors, and also for arbitrary triples of squares. These statistical equivalences are crucial in the analysis of the receptive-field properties of neurons that respond differentially to the two ensembles.

In addition to the isodipole-16 stimulus, standard contrast–reversal and appearance–disappearance checkerboard stimuli were used. For these stimuli, the checkerboard was constructed on the same lattice as the isodipole stimuli.

The stimuli described above were realized on a Tektronix 608 display oscilloscope with a fast white (P4) phosphor driven by specialized electronics interfaced to a PDP 11/23 computer (7). This apparatus provided for control of a 256 × 256 pixel raster display at a frame rate of 270.3 Hz. The raster has a mean luminance of 100 candela (cd)/m$^2$ and a display area of 23° × 23° at the viewing distance of 25 cm. The check size was 43 min (8 × 8 pixels), so that a 32 × 32 swatch of each texture was displayed. Each phase of the stimulus was displayed for one-half of the 947-msec period; thus, the complete even–odd, contrast–reversal, or appearance–disappearance cycle was presented at a rate of 1.056 Hz. The contrast of the stimulus (fractional deviation of the luminance of the bright squares above the mean luminance, and of the dark squares below the mean luminance) was 0.3.

Simultaneous recordings of single unit activity in the LGN and multiple unit activity in the LGN and the VEP were made in three anesthetized paralyzed adult male and female cats. Eight LGN X cells and four LGN Y cells were studied. The basic physiological preparation was standard (8). Surgical anesthesia was induced and maintained with sodium thiamylal. Subsequently, paralysis and anesthesia were maintained with gallamine triethiodide (5 mg·kg$^{-1}$·hr$^{-1}$, i.v.) and urethane (0.2 g/kg, i.v. loading; 0.1 g·kg$^{-1}$·24 hr$^{-1}$, i.v. maintenance). No recordings were made until at least 4 hr had elapsed since the last administration of sodium thiamylal.

A Ringer-filled microelectrode (10–20 MΩ) was advanced vertically through a burr-hole in the skull until the extracellularly recorded action potential of a single neuron in the dorsal LGN could be reliably discriminated by its height

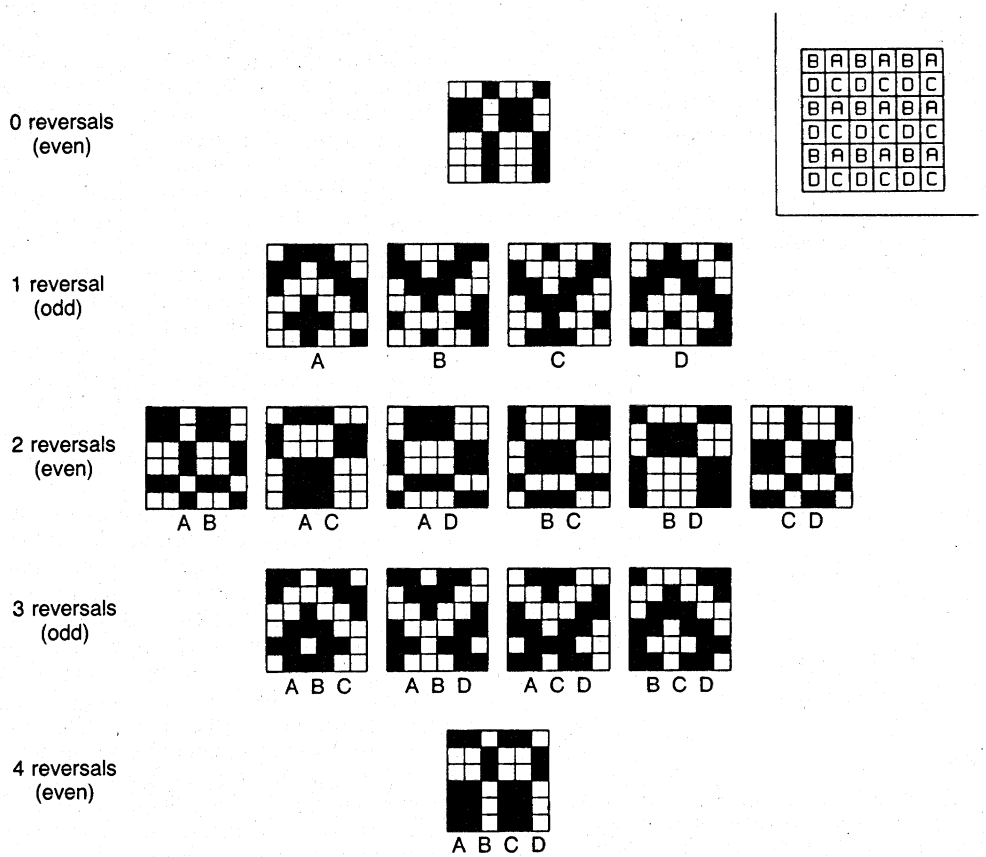


FIG. 2. Derivation of eight even textures and eight odd textures from a single even texture. (*Inset*) A partition of the square lattice into four sets of squares. In each row of the main figure, the states of the squares that lie in a fixed number of the sets (A, B, C, and D) defined in the *Inset* are reversed. Reversal of an odd number of sets of squares produces an odd texture; reversal of an even number of sets of squares produces an even texture. The texture in the top row corresponds to the even texture of Fig. 1; the first texture in the second row corresponds to the odd texture of Fig. 1.

above the background neural activity. The receptive field of the unit was mapped on a tangent screen, and the unit was classified as X or Y by its response to a high spatial frequency grating (8). Refraction was corrected by trial lenses chosen to optimize the unit's response to fine patterns. For combined VEP/single unit recording, only units in the central 10° of vision were used. Thus, the visual display could be centered over the area centralis and simultaneously cover the receptive field of the unit. The contralateral eye was occluded, and the remainder of the visual field was dark. During recording, one discriminator circuit was set to send pulses to the computer at each occurrence of an action potential of the unit under study. A second discriminator circuit was set with its criterion at a lower voltage, so that a pulse would be sent to the computer at each occurrence of either the action potential of the single unit or any of the much smaller action potentials recorded by the microelectrode from several neighboring units. The EEG was recorded bipolarly from screw electrodes at Horsley–Clarke coordinates (−3A, 0L) and (20A, 0L). After 10,000-fold amplification and bandpass filtering (0.03–300 Hz), the signal was fed to an analog-to-digital converter and the computer, which averaged the response over the stimulus cycle. The EEG was sampled every frame of the display, approximately every 3.7 msec. Each stimulus type was presented for three or four episodes of 2 min each.

## RESULTS

Fig. 3 shows simultaneous recordings of the average firing rate of a cat LGN Y cell, a cluster of nearby single units, and the VEP. In addition, the response of a cat LGN X cell recorded under identical conditions in a separate preparation is shown.

The X cell response to the isodipole-16 stimulus shows only a small depression of the firing rate following each stimulus transition, and the responses at the two transitions are similar. The response of this cell to contrast–reversal and appearance–disappearance is more prominent. For each of these stimuli, the responses at the two transitions are qualitatively different: an overall pattern of excitation followed by inhibition at the first transition, and an overall pattern of inhibition followed by excitation at the second transition. The

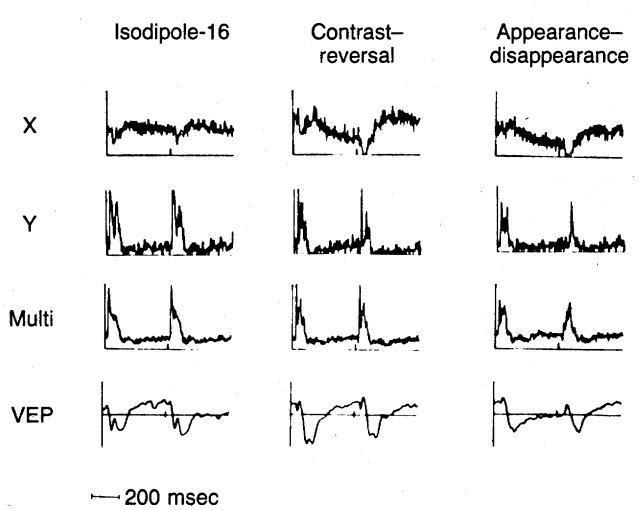


FIG. 3. Single-unit, multiunit, and evoked potential response to three stimulus types. The Y cell activity (off-center; unit 15/6), the multiunit activity, and the evoked potential activity were recorded simultaneously; the X cell (on-center; unit 14/2) was recorded in a separate preparation. The stimulus period (horizontal full scale) is 947 msec. Vertical calibration (full scale) X cell, 50 impulses per sec; Y cell, 20 impulses per sec; multiunit activity, 120 impulses per sec; VEP, 60 μV; upward deflection indicates negativity at the occipital electrode.

Y cell response has a burst of activity at each transition of all three stimuli. The multiunit cluster recorded from the same electrode shows a similar pattern. Within each stimulus type, the time course of the excitatory burst was roughly the same at the two transitions, but the detailed firing pattern varies across the three stimuli.

The VEP elicited by all three stimuli has a wave of occiput positivity (downward deflection) beginning 60–100 msec after each stimulus transition. The detailed shape of this early response differs from stimulus to stimulus. However, within each stimulus type, a similar waveform is observed at the two transitions.

For the contrast–reversal stimulus, the VEP responses to each of the two transitions are identical. But this behavior is not observed in the other two stimuli. For the isodipole-16 stimulus, there is a prolonged negativity at the occiput (upward deflection) observed following the transition to the even textures (first half of the stimulus cycle). This wave is not present following the transition to the odd textures (second half of the stimulus cycle). Exactly the opposite behavior occurs in response to the appearance–disappearance stimulus. However, asymmetry in response to the appearance–disappearance stimulus is variable both within and across preparations.

The above responses were decomposed into two components, a symmetric component and an antisymmetric component (Fig. 4). The symmetric component is defined as the average of the responses to the two transitions of each stimulus. The antisymmetric component is defined as the difference between the actual response and the symmetric component. For ease of interpretation, the antisymmetric components of the single unit and multiunit responses are plotted in Fig. 4 after upward displacement by an amount equal to the mean rate.

This decomposition has several useful properties. If the actual responses to both transitions are equal, the symmetric component is equal to the actual response and the antisymmetric component is zero. If the actual responses to both transitions are identical in shape but opposite in sign, the symmetric component is zero and the antisymmetric component is equal to the actual response. A response that is intermediate between these two extremes (an asymmetric response) is nevertheless equal to the sum of its symmetric and antisymmetric components; the size and shape of these components define the elements of the response that are present at both transitions (the symmetric component) and those that are not (the antisymmetric component).

It is clear from Fig. 4 (*Left*) that all VEP responses have large symmetric components. However, the antisymmetric component of the pattern reversal response is much smaller than the antisymmetric component of the isodipole-16 response. The antisymmetric response isolates the difference in processing of the even and the odd textures.

To determine the source of the antisymmetric response, it is crucial to examine the concomitant neural activity in the LGN. The antisymmetric components of LGN responses to the isodipole-16 stimulus are shown in the first column of Fig. 4 (*Right*). There is no apparent antisymmetry in the X cell response to the isodipole-16 stimulus. The antisymmetric component of the Y cell response has a brief transient (1 bin or 3 msec). Even this minimal antisymmetry is not present in the response of the multiunit cluster, which shows no detectable antisymmetric response to the isodipole-16 stimulus.

The size of the antisymmetric response may be quantitated by the fraction of the total power that is contained in the odd harmonics. For the isodipole texture, this fraction was 24.9% for the VEP, 6.7% for the X cell, 2.1% for the Y cell, and 0.3% for the multiunit cluster of Fig. 3. In all preparations, a similarly small antisymmetric response component to the isodipole-16 stimulus was observed at the level of the LGN, while a clear

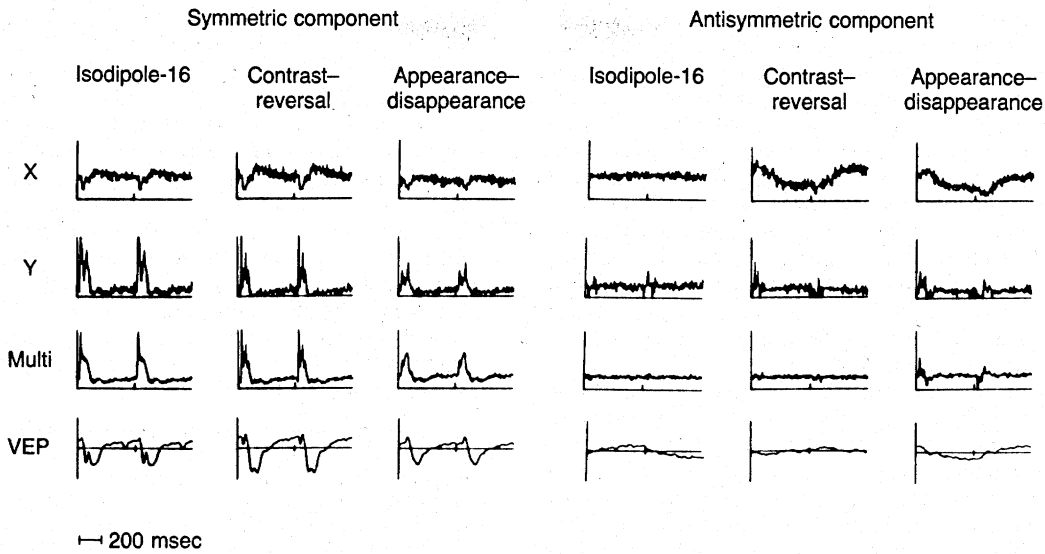


FIG. 4. Analysis of asymmetric and antisymmetric components of single-unit, multiunit, and evoked potential responses shown in Fig. 3. (*Left*) Symmetric component. (*Right*) Antisymmetric component. Scales are the same as in Fig. 3.

antisymmetric response was simultaneously recorded in the VEP. Thus, the antisymmetric component of the VEP is not a direct manifestation of precortical processing.

Conversely, single neuron activity in response to contrast reversal often shows an antisymmetric component: for example, the X cell in Fig. 4 (*Right*). However, the contrast–reversal VEP shows only a minimal antisymmetric component, because it is an average of responses over a wide area of the visual field, which contains an approximately equal number of elements undergoing contrast–reversal in opposite directions. Thus, antisymmetric responses of single neurons have canceled upon averaging over the visual field and are not registered in the VEP.

The appearance–disappearance responses present yet a third behavior. An antisymmetric response component is registered in many precortical neurons (the X cell, the Y cell, and the multiunit recording shown in Fig. 4). Symmetry considerations do not force cancellation of these responses when averaged over the entire stimulus, and thus precortical processes contribute to the antisymmetric component of the appearance–disappearance VEP.

## DISCUSSION

The present approach separates the VEP into components based on the nature of the neural interactions that generate the response. A VEP is elicited by interchange between two classes of visual textures. For the antisymmetric component of the response to separate complex processing from more simple stages, it is necessary for the two classes of textures to be balanced in their ability to drive neurons whose receptive fields are relatively simple. The stimulus used in previous VEP studies (5, 6) consisted of interchange between a single even and odd texture; this balance held only after an average over space. In the present study, in which single unit and VEP responses are compared, this balance must be maintained separately for neurons centered at every point in the visual field, after an average over time. This condition is satisfied by the isodipole-16 stimulus. In humans, the isodipole-16 stimulus and simple even/odd interchange elicit similar VEPs. Thus, the replacement of the spatial average by the temporal average provides for a more direct comparison with single unit activity without affecting the VEP. We will demonstrate that the antisymmetric component of the isodipole-16 VEP isolates intracortical processing, while the antisymmetric component of the appearance–disappearance VEP likely has contributions from both precortical and intracortical phenomena. The symmetric component of the VEP elicited by the three stimulus types studied here is also a mixture of cortical and precortical influences.

**Analysis of the Source of Symmetric and Antisymmetric Components.** Consider first a neuron that is driven by the luminance at a given point in the field. In response to the checkerboard contrast–reversal stimulus, the firing rate of a hypothetical "luminance" neuron should be equal and opposite at the two transitions of the stimulus cycle. However, this antisymmetry will not result in a net antisymmetry in the VEP, because an equal number of points are brightening and darkening at each transition.

A similar analysis holds for the response of luminance units to appearance–disappearance. Single units would be expected to show a difference in response at the two transitions of the stimulus cycle. However, an average over a population of such neurons would have no antisymmetric response component, provided only that responses to decrements in light are the exact inverses of responses to increments in light. This is a consequence of linearity.

The isodipole-16 stimulus also would not be expected to evoke an antisymmetric response component from luminance units. This is because any given point of the field has the same average luminance over time for both the even and the odd textures, and bright-to-dark and dark-to-bright transitions are equally likely. Thus, although an antisymmetric response component may be generated by transitions between a particular pair of even and odd textures, no antisymmetry in response can be maintained in a time average over the entire sequence of transitions (the isodipole-16 stimulus).

This analysis for hypothetical luminance neurons extends to real neurons whose receptive fields are composed of linearly summing pools (such as the center and surround), whose activities combine without further interaction. The detailed size and shape of the receptive field elements are irrelevant as long as spatial summation is linear. In particular, individual X cells of the cat retina and LGN (8–13) would be expected to manifest an antisymmetric response to the checkerboard stimuli but not the isodipole-16 stimulus (Fig. 4). For all three stimuli, an average across the X cell population will not result in an antisymmetric VEP component. A similar behavior is to be expected from the ≈90% of both the tonic and phasic geniculate neurons of the monkey, which are qualitatively linear (14, 15).

Next, consider an idealized "contrast" neuron whose receptive field structure includes an interaction in which

signals representing the deviation in light intensity from background at two locations are multiplied. If these two locations overlap, the resulting signal increases with increasing deviation of light intensity from background but is insensitive to whether the change is a brightening or a darkening. If these two locations are nonoverlapping or if the interaction follows (linear) lateral inhibitory interactions, the resulting signal reflects spatial contrast. The analysis of responses of such idealized contrast neurons given below applies equally well to more complex spatial interactions (5).The Y class of cat retinal and LGN neurons (12, 16, 17), and the monkey LGN neurons with similar spatial properties (15), may be considered as a combination of contrast neurons and the linear neurons treated above.

A contrast neuron will be stimulated equally at both phases of checkerboard pattern reversal, since it is sensitive to deviations from the mean luminance but insensitive to the direction of the change. The predominantly symmetric Y cell response to contrast–reversal, as shown in Fig. 4, is an example of such a response; the antisymmetric component (which is present in single unit responses but not in the VEP) reflects the contribution of linearly summing receptive field elements. The symmetric contributions of contrast neurons will reinforce when averaged over the visual field, and, therefore, contrast neurons will contribute a symmetric component to the checkerboard contrast–reversal VEP (18). Similarly, the symmetric component of the X cell response to this stimulus is likely a manifestation of minor nonlinearities in the receptive-field structure of the X cell.

The response of contrast neurons to appearance–disappearance is qualitatively different. In one phase of the stimulus (pattern present), there is ample spatial contrast. In the other phase (pattern absent), there is no spatial contrast. Thus, contrast neurons are likely to generate an asymmetric response to appearance–disappearance. The antisymmetric component of this response will not cancel upon summation across neurons scattered over the visual field (Y cell and multiunit responses in Fig. 4). Thus, the resulting VEP will contain a net antisymmetric component. Although this argument indicates that precortical processes lead to an antisymmetric component in the appearance–disappearance VEP, an additional contribution from cortical processes may be present as well (19).

The appearance of the isodipole-16 stimulus is dramatically different at the two phases of the stimulus cycle (Figs. 1 and 2). One might expect, therefore, that a contrast neuron, which is sensitive to basic aspects of the pattern, will generate an asymmetric response to this stimulus. However, the statistical properties of the stimulus guarantee that this cannot occur. For example, the even and odd textures contain an equal number of pairwise juxtapositions of a bright and a dark square. Furthermore, in both textures, the likelihood of a bright and a dark square occurring at any relative displacement is equal. Formally, this can be expressed by the statement that the spatial power spectra of the two texture ensembles are identical [the isodipole condition (4)]. These equivalences suffice to guarantee that the contribution of a contrast neuron to this stimulus will be symmetric and that no antisymmetric component will be present (5). Thus, although the even and odd textures look quite different, neither X nor Y cells respond in a differential fashion to these texture ensembles (Fig. 4).

Monkey LGN cells have broadly similar receptive-field properties, although the correspondence of cell classes with the cat X/Y dichotomy is unclear (14, 15). Psychophysical studies indicate close parallels between the early visual systems of human and macaque (20, 21). Since the present analysis is based on the major qualitative features of receptive-field structure, we conclude that in humans, the antisymmetric component of the VEP response to the isodipole-16 stimulus is not of precortical origin.

The major nonlinearity in both simple and complex cells appears to be rectification (22–25). Rectification is unlikely to be responsible for the isodipole-16 antisymmetric response component, although it may well contribute to the antisymmetric response component elicited by appearance–disappearance and to the symmetric response component to all three VEP stimuli (5, 6). Neurons with receptive fields sufficiently complex to contribute to the isodipole-16 antisymmetric response include hypercomplex cells (26) and middle temporal cells that are sensitive to nonlinear combinations of spatial frequency components (27). However, in the absence of a detailed receptive-field model or further experimental evidence, their role must be considered hypothetical.

I am grateful for the discussions with Ehud Kaplan, Bruce Knight, Floyd Ratliff, Robert Shapley, and Vance Zemon, and for the excellent technical support of Mary Conte, Yvonne Holland, Norman Milkman, Michelangelo Rossetto, and Gary Schick. This work was supported by grants from the National Institutes of Health, The Harry Frank Guggenheim Foundation, The Hartford Foundation, the McKnight Foundation, and Mrs. Wolfgang Schoenborn.

1. Tyler, C. W., Apkarian, P. A. & Nakayama, K. (1978) *Exp. Brain Res.* **33,** 535–550.
2. Kooi, K. A. & Marshall, R. T. (1979) *Visual Evoked Potentials in Central Disorders of the Visual System* (Harper & Row, Cambridge, England).
3. Zemon, V. & Ratliff, F. (1982) *Proc. Natl. Acad. Sci. USA* **79,** 5723–5726.
4. Julesz, B., Gilbert, E. N. & Victor, J. D. (1978) *Biol. Cybern.* **31,** 137–140.
5. Victor, J. D. (1985) *Vision Res.* **25,** 1811–1827.
6. Victor, J. D. & Zemon, V. (1985) *Vision Res.* **25,** 1829–1844.
7. Milkman, N., Schick, G., Rossetto, M., Ratliff, F., Shapley, R. & Victor, J. (1980) *Behav. Res. Methods Instrum.* **12,** 283–292.
8. Hochstein, S. & Shapley, R. M. (1976) *J. Physiol. (London)* **262,** 237–264.
9. Victor, J. D. & Shapley, R. M. (1979) *J. Gen. Physiol.* **74,** 275–298.
10. Rodieck, R. W. & Stone, J. (1965) *J. Neurophysiol.* **28,** 819–832.
11. Rodieck, R. W. & Stone, J. (1965) *J. Neurophysiol.* **28,** 833–848.
12. Enroth-Cugell, C. & Robson, J. G. (1966) *J. Physiol. (London)* **187,** 517–552.
13. Enroth-Cugell, C. & Pinto, L. (1970) *Nature (London)* **226,** 458–459.
14. Dreher, B., Fukuda, Y. & Rodieck, R. W. (1976) *J. Physiol. (London)* **258,** 433–452.
15. Kaplan, E. & Shapley, R. M. (1982) *J. Physiol. (London)* **330,** 125–143.
16. Hochstein, S. & Shapley, R. M. (1976) *J. Physiol. (London)* **262,** 265–284.
17. Victor, J. D. & Shapley, R. M. (1979) *J. Gen. Physiol.* **74,** 671–689.
18. Spekreijse, H., Van der Tweel, L. H. & Zuidema, T. (1973) *Vision Res.* **13,** 1577–1601.
19. Nakayama, K. & Mackeben, M. (1982) *Vision Res.* **22,** 1261–1271.
20. De Valois, R. L., Morgan, H., Polson, M. C., Mead, W. R. & Hull, E. M. (1974) *Vision Res.* **14,** 53–67.
21. De Valois, R. L., Morgan, H. & Snodderly, D. M. (1974) *Vision Res.* **14,** 75–81.
22. Movshon, J. A., Thompson, I. D. & Tolhurst, D. J. (1978) *J. Physiol. (London)* **283,** 53–77.
23. Movshon, J. A., Thompson, I. D. & Tolhurst, D. J. (1978) *J. Physiol. (London)* **283,** 79–99.
24. Spitzer, H. & Hochstein, S. (1985) *J. Neurophysiol.* **53,** 1244–1265.
25. Spitzer, H. & Hochstein, S. (1985) *J. Neurophysiol.* **53,** 1266–1286.
26. Kato, H., Bishop, P. O. & Orban, G. A. (1978) *J. Neurophysiol.* **41,** 1071–1095.
27. Movshon, J. A., Adelson, E. H., Gizzi, M. S. & Newsome, W. T. (1985) *Pontif. Acad. Sci. Scr. Varia* **54,** 117–151.